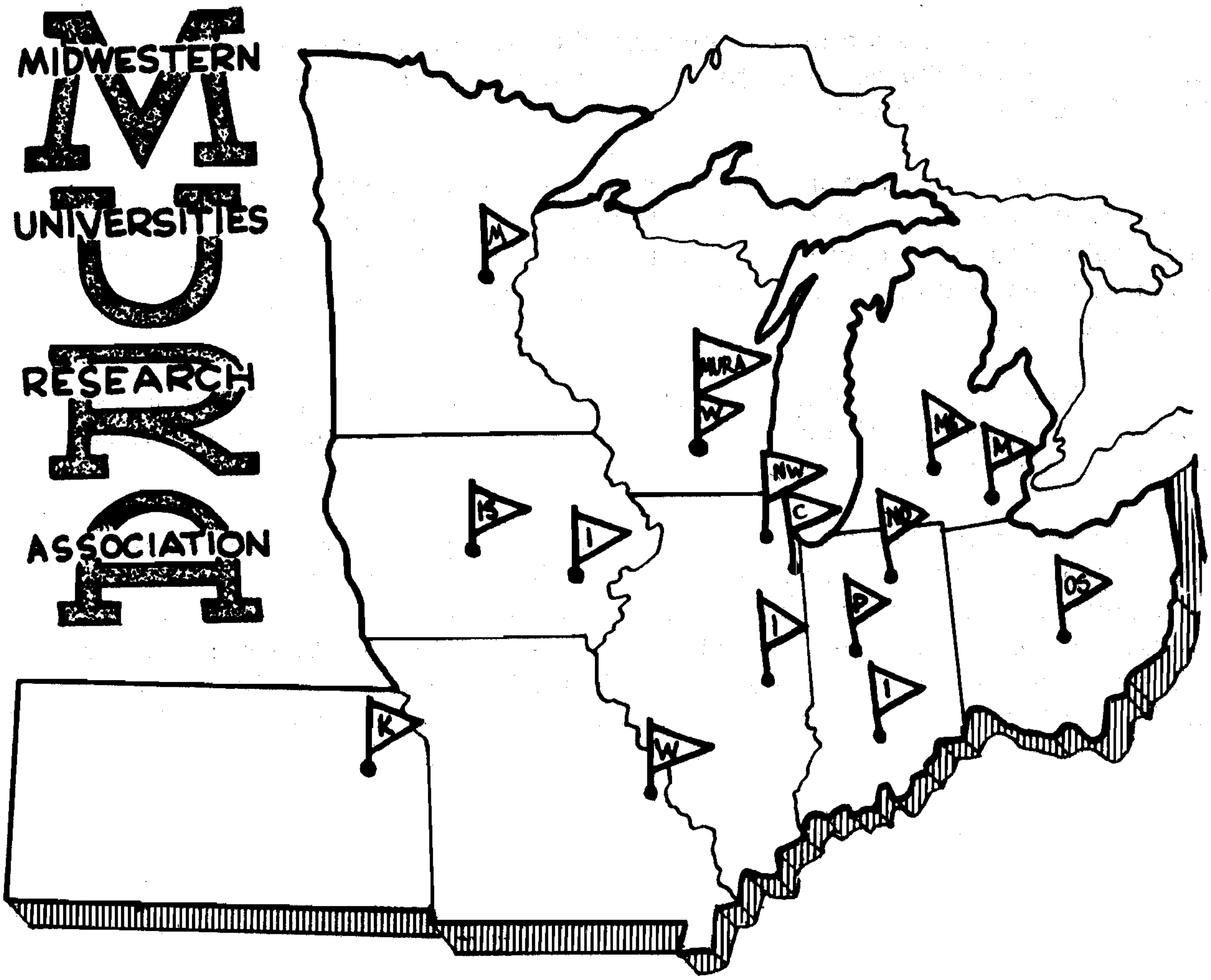

A LOW FIELD SUPERCONDUCTING FFAG MODEL MAGNET

G. del Castillo

REPORT NUMBER 709

Printed in USA. Price $0.50. Available from the

Office of Technical Services
U. S. Department of Commerce
Washington 25, D. C.

CONTENTS

I. INTRODUCTION 3

A. General 3
B. Fixed Field Alternating Gradient Accelerators 4

II. THEORY OF A SUPERCONDUCTING MAGNET 5

A. Early Attempts 5
B. The First Model 10

III. EXPERIMENTAL PROCEDURES 14

A. Analog Magnet 14
B. The Superconducting Magnet 17

i) Cryogenic System 17
ii) The Field Measuring Probe 20
iii) The Magnet 22
iv) Results 25

IV. RECENT DEVELOPMENTS AND CONCLUSIONS 28

V. ACKNOWLEDGEMENTS 32

VI. REFERENCES 33

MURA-709
UC-28: Particle Accelerators and
High-Voltage Machines
TID-4500 (37th Edition)

MIDWESTERN UNIVERSITIES RESEARCH ASSOCIATION*

P. O. Box 6, Stoughton, Wisconsin

A LOW FIELD SUPERCONDUCTING FFAG MODEL MAGNET

G. del Castillo

February 26, 1965

ABSTRACT

The possibility of using superconducting surfaces for shaping a magnetic field to have the required H vs r dependence in a magnet of the type used in a radial sector FFAG accelerator is demonstrated for fields below 2 kG. The theoretical results of using superconducting surfaces were confirmed first by using an audio-frequency analog model where the electric skin effect plays the role of the Meissner effect for the superconductor. A study made on different coil-plate geometries indicated that it is possible to obtain exponential fields of the type $H = H_o \exp K/r_o \cdot x$. The results obtained with an actual superconductor agree with those of the audio-frequency analog, thus proving that, up to a 2 kG field, (a) it is possible to shape the magnetic field by superconducting surfaces, (b) modeling studies can be made using an audio-frequency analog.

The helium dewar system used in this work makes use of the cold He gas to establish a suitable temperature gradient from room temperature to

*AEC Research and Development Report. Supported by the U. S. Atomie Energy Commission through ANL by Subcontract 31-109-38-1707.

4° K to minimize He losses. The probe for measuring the magnetic field at He temperature is a bismuth fiber which presents the characteristics of a single crystal. Fiber voltage sensitivities varied from 5 to 30 volts/gauss-mA, giving an accuracy of about 0.1% when used with a dc amplifier and digital voltmeter system.

I. INTRODUCTION

A. General

The application of superconductors to magnet components suitable for use in particle accelerators has, in the past, been delayed for two main reasons. First, the critical fields observed by de Hass, Mendelssohn, Voogd[1] and others in their pioneering work were rather low, well within the range covered very successfully by iron core magnets without the complications inherent in working at low temperatures. Second, the technology of producing and handling liquid He in large quantities was not quite developed.

Only in the last few years, with the discovery of the high critical field superconductor[2, 3] and the improvement in the technology of handling liquified gases, one is in a position of thinking in applying superconductors to something different from high field solenoids now used for research purposes. A possible application may be in the field of high energy physics; this work, as carried in the present laboratories, seems to be moving in the direction of using particle accelerators of higher energies. This means that regardless of the type of accelerator in question large amounts of power are required not only to energize the guide fields but also for conducting experiments. Furthermore, in some accelerators such as the spiral sector FFAG[4, 5] the problem is still enhanced due to the extended and complicated nature of the magnetic field.

Although the possibility of using superconducting materials for an accelerator magnet is at present limited to time independent fields, their use in such machines may represent a solution to the power problem. However, it seems unlikely that this fact alone can justify their application in an accelerator. Compactness, simplicity and reliability may be important features demanded in future accelerators. The use of superconducting surfaces to shape the magnetic field is a step in this direction.

There are still several problems involved, not only regarding the technical difficulties of working at low temperature, but also some of a more fundamental nature, concerning our present knowledge of the electrodynamics of the high critical field superconductors. In this respect considerable work is being done to better understand the properties of such materials,[6] as well as to develop fabrication procedures which will allow achievement of higher critical fields in larger volumes.[7] The possible use of superconductors in an accelerator appears to be a motivation for future developments both in techniques and basic research. This may apply to the work done in radiation effects on superconductors[8, 9] and their corresponding interpretation.[10] This subject, however, is still an open question when dealing with particle flux and energy existing in an accelerator.

B. Fixed Field Alternating Gradient Accelerators

Among the cyclic particle accelerators that use a time independent guide field, the FFAG has demonstrated its importance by achieving high circulating currents, long duty cycle and versatility in its operation.[11] These machines can be either the radial or spiral sector type.[4] In a radial sector machine the field at the median plane is given by $H = H_o (r/r_o)^k$ [(*)] where subindex zero refers to reference field and radius, r is the distance from the center of the

---

[(*)] A complete description of the field should include the azimuthal variation, in this case is omitted for simplicity.

machine to the equilibrium orbit, and the field index $k = R/H \cdot dH/dR$. The only operating machine of this type is the MURA 50 MeV electron model.[11] The magnetic guide field consists of 32 magnets each having opposite sign in the direction of field. The field measured along the radius and at the center of each magnet satisfies the above equation.

The required variation of field vs. radius is accomplished by distributing windings along the inner surfaces of the iron which are slotted to accommodate the coils. The final trimming of the field is made by means of pole face windings.

The work that follows is an attempt to produce the magnetic field required by an FFAG magnet by using superconductors. The results that have been obtained are not yet applicable to high magnetic fields, first because our incomplete knowledge of the Type II superconductor electrodynamics prevents us from making predictions and second, lack of more realistic experimental results. Further studies simulating radiation effects, magnetic forces and field interactions between the different magnets may decide whether the present work may be applied to an accelerator.

II. THEORY OF A SUPERCONDUCTING MAGNET

A. Early Attempts

The first solution to the problem of demonstrating the possibility of obtaining an exponential field by using a combination of currents and superconducting plates was given by Van Bladel.[12] In his treatment he demonstrates that the magnetostatic potential ψ resulting from a current distribution in the presence of a superconducting surface is equivalent to the electrostatic potential ϕ of a volume density of charge in the presence of an uncharged conductor. The equipotentials are equivalent to the lines of force of the magnetic problem. Thus the magnetic field components are given by the normals to the corresponding electric components derived from the potential.

The "geometry" used by Van Bladel appears in Fig. 1. The sources of a density $\rho(r, \varphi)$ are distributed symmetrically with respect to the axis $\varphi = 0$, the superconducting surfaces meet at $r = 0$. The region where the field should obey an exponential law is determined by the plates and the sources.

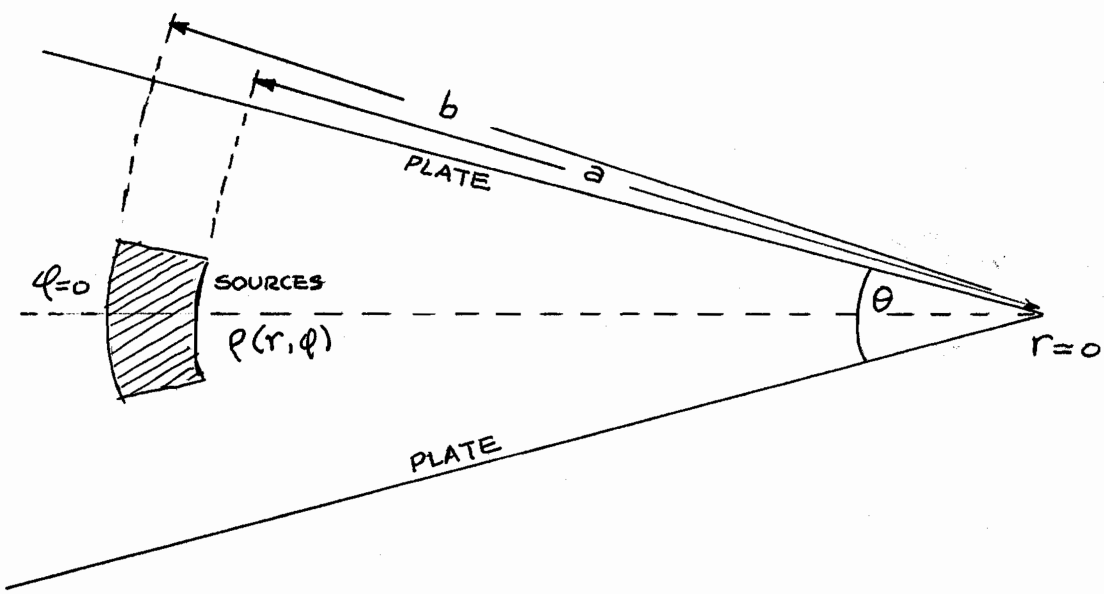

FIG. 1

The solution of Poisson's equation in the region $r < a$ is given by

$$\Phi = -\frac{\theta}{2\pi} \sum_{1,3..}^{n} r^{\frac{n\pi}{\theta}} \cos\frac{n\pi\varphi}{\theta} \left[\frac{A_n}{n} \int_a^b \frac{\rho(r')}{(r')^{n\pi/\theta}} dr' \right]$$

where

$$A_n = \frac{2}{\theta} \int_{-\theta/2}^{+\theta/2} F(\varphi) \cos\frac{n\pi\varphi}{\theta} d\varphi \quad ; \quad F(\varphi) = \text{charge distribution}$$

the angles θ and φ are illustrated in the figure.

The exponential field r^k is obtained by choosing $\theta = \frac{n\pi}{k}$ and for the variation of the charges $\cos \frac{n\pi\varphi}{\theta} = \cos k\varphi$.

A more practical configuration, as we shall see later, is shown in Fig. 2. This is the case of two line sources symmetrically located with respect to axis. The potential in the region $0 < r < 1$ is expressed by

$$\phi = -\sum_{1,3}^{n} \frac{1}{n\pi} \cos\left(\frac{n\pi}{2}\frac{\alpha}{\theta}\right) r^{\pm\frac{n\pi}{\theta}}$$

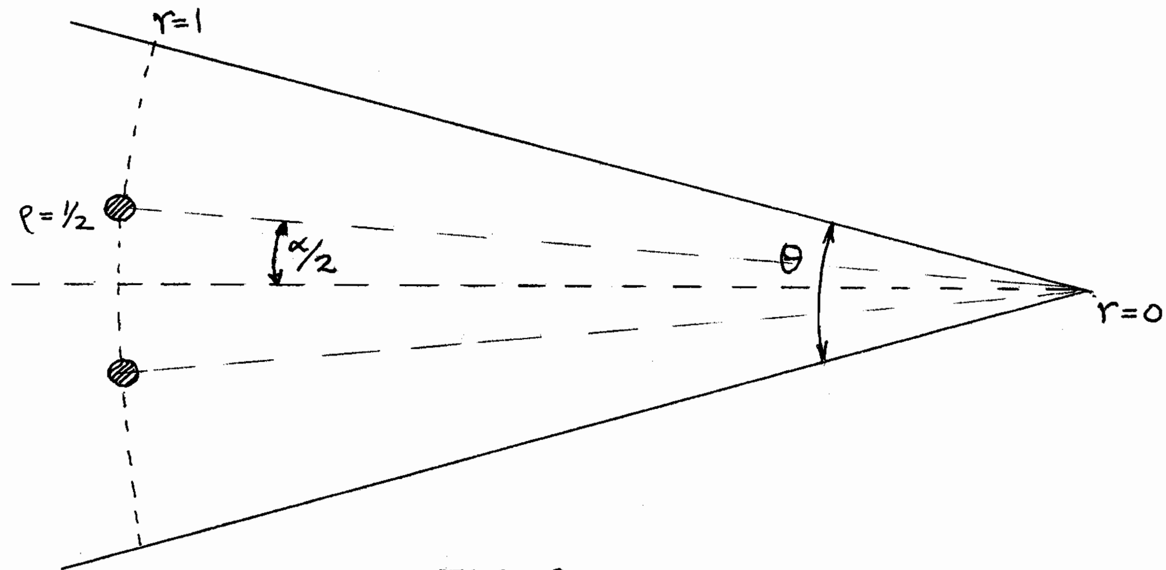

FIG. 2

The plots for different values of α/θ are given in Figs. 3 and 4. They show a portion where the r^k law holds. Near the sources, at $r \approx 0.6$, the exponential variation is no longer valid.

The conclusion of this work is that in principle it is possible, by a suitable selection of currents and superconducting plates, to obtain magnetic fields that obey a certain law, which in this case is r^k as needed for the FFAG radial sector magnet.

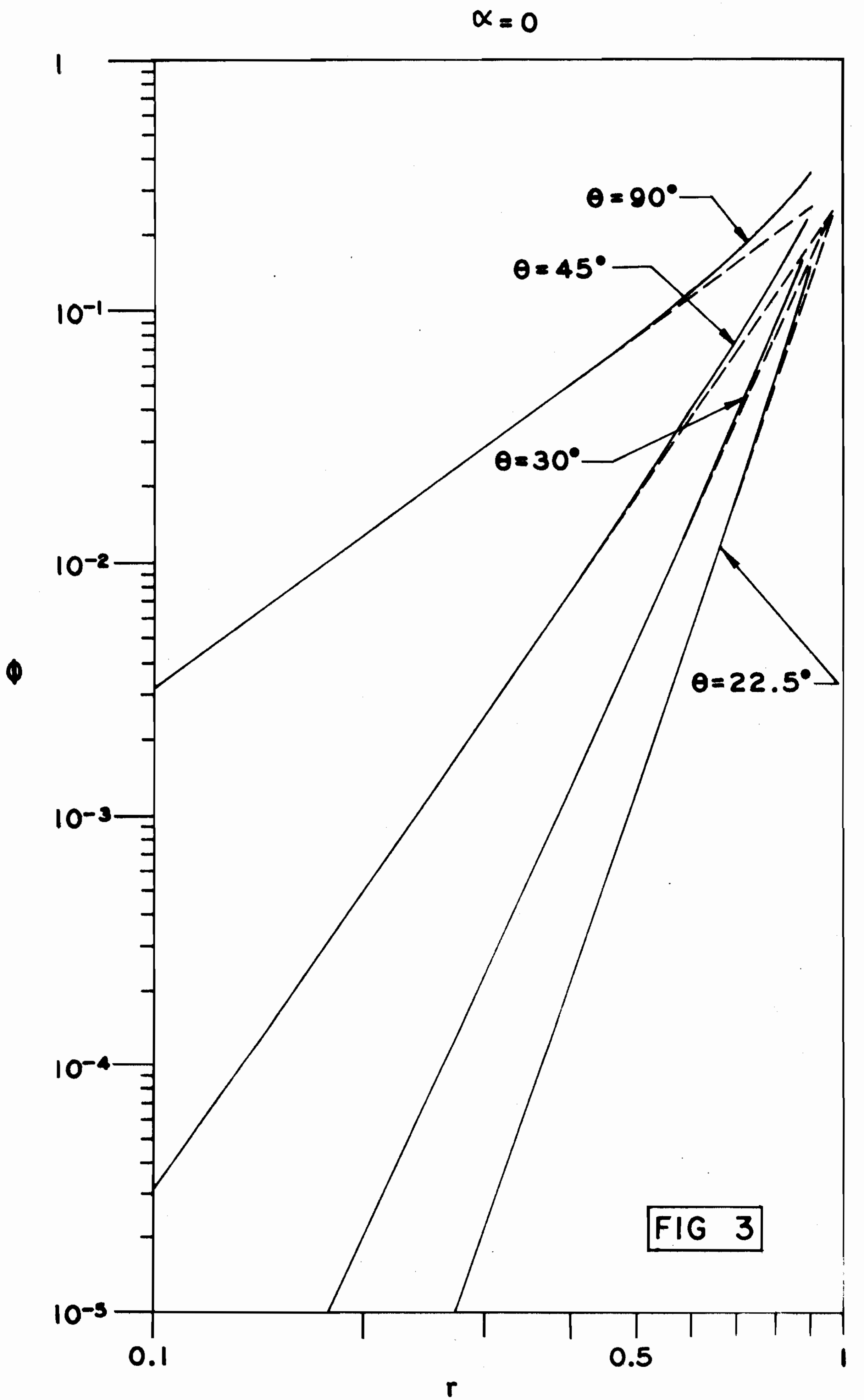

FIG 3

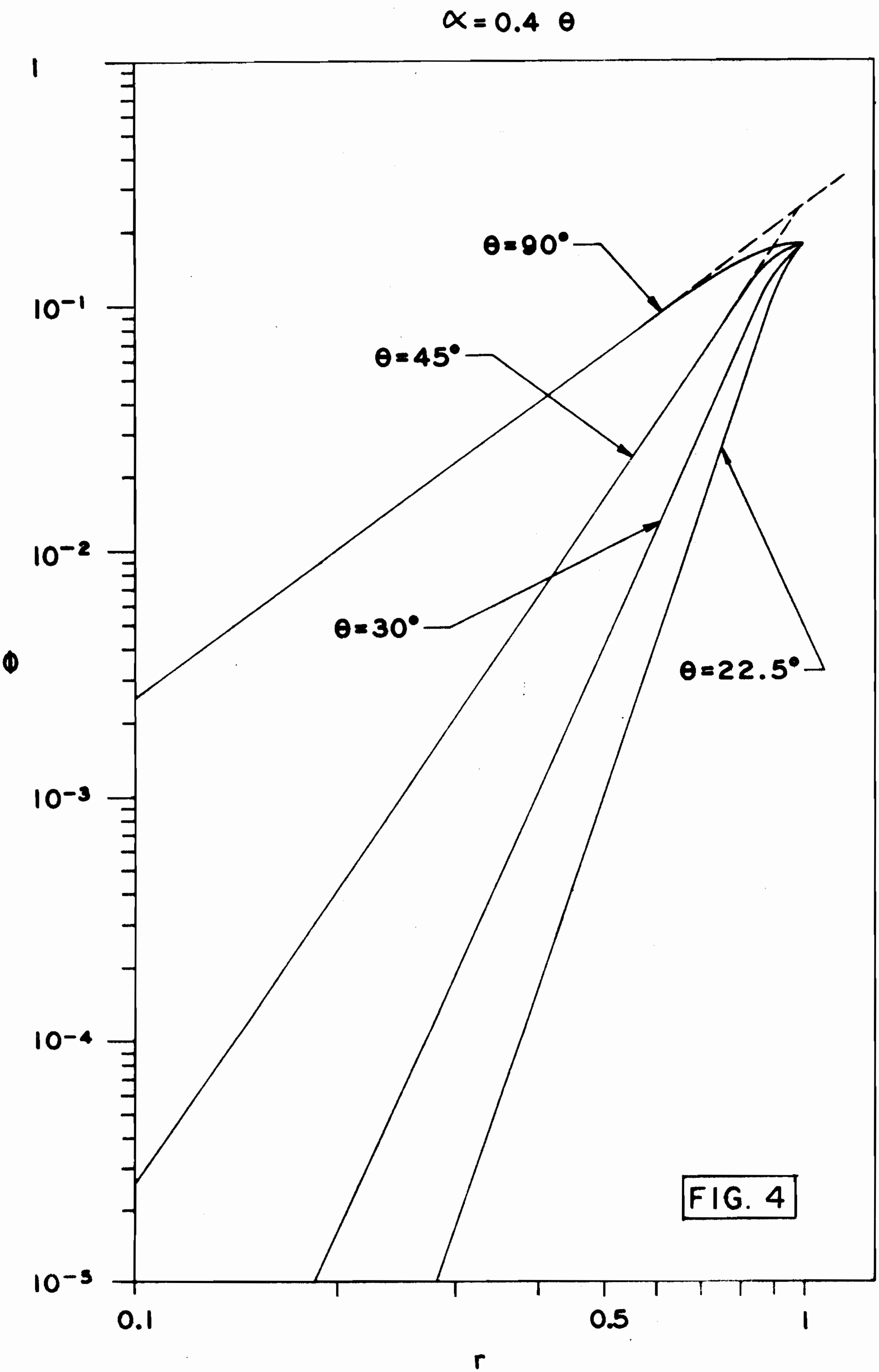

FIG. 4

Van Bladel's results agree in certain ways with the results that Symon[13] had previously obtained in a study of a superconducting FFAG accelerator, except that it was thought by the author that Symon's current distribution could be replaced by a surface of a superconductor that exhibits a Meissner effect. This, in fact, motivated Van Bladel's work.

B. The First Model[14]

An experimentally feasible arrangement of currents and superconducting surfaces, which has some of the features required in an FFAG accelerator magnet, appears in Fig. 5. A coil of superconducting material is wound around a prism-shaped form, the end result being a bundle of conductors of approximately circular cross section running along the front edge of the prism and their returns distributed in slots in the back surface.* Two superconducting plates are located above and below the prism.

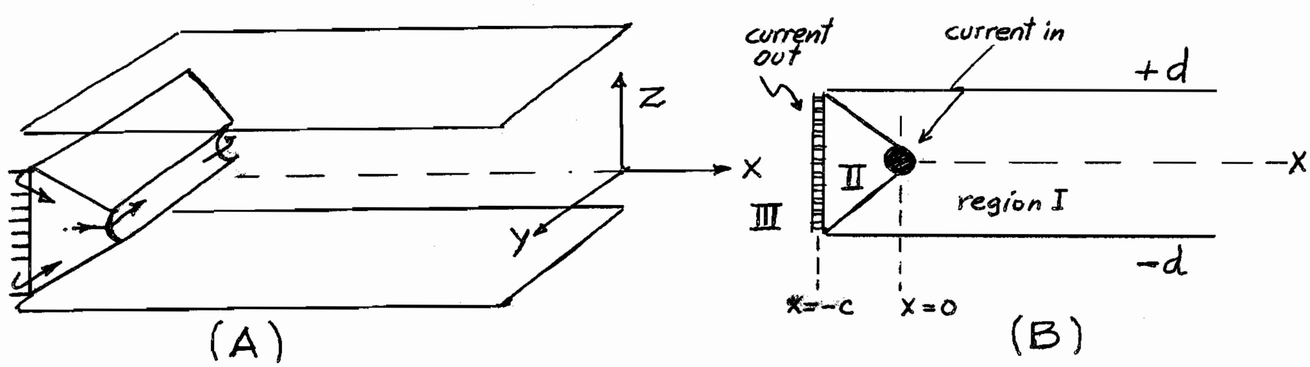

FIG. 5

*Actual photograph of this configuration is shown in Fig. 13.

In the ideal case of an infinitely long prism, the field at the median plane, resulting from the coil alone, is given in a first approximation by

$$H_z \doteq \frac{1}{x} - \frac{1}{x+c}$$

The presence of the plates will modify this dependence mostly by decreasing the value of the vertical components of the field. This comes as a consequence of the Meissner effect. The result is such that the field produced by the currents in the coil will induce a supercurrent in the plates, to cancel the normal components of the field at the surface of such plates. The current distribution resulting from this configuration is, in a way, equivalent to the distributed windings in the iron magnet, except that the supercurrent distribution is much finer, approximating the ideal case of a continuous distribution. Otherwise the magnets are similar, the magnetic properties of iron being replaced by the magnetic behavior of a superconductor.

The plate and coil configuration, described above, is represented schematically in Fig. 5b. It is divided in regions I, II, and III; region I is the one of interest.

The solution of Laplace's equation satisfying the boundary condition that the normal component of the field vanish at the surface of the plates is, for regions I, II and III, given by

$$V_{I} = \sum^{n} A_n e^{-\mu_n x} \sin \mu_n z$$

$$V_{II} = \sum^{n} \left\{ B_n e^{\mu_n x} + C_n e^{-\mu_n x} \right\} \sin \mu_n z$$

$$V_{III} = \sum^{n} D_n e^{\mu_n x} \sin \mu_n z$$

with $\mu_n = \frac{(2n+1)\pi}{2d}$

By matching the values of the normal and tangential components of H in the three regions, taking into account the singularities at the sources, the following relations between the coefficients are obtained.

$$-A_n = B_n - C_n$$

$$\mu_n d\left[A_n - B_n - C_n\right] = 4\pi I$$

$$B_n e^{-\mu_n c} - C_n e^{\mu_n c} - D_n e^{-\mu_n c} = 0$$

$$-D_n e^{-\mu_n c} + B_n e^{-\mu_n c} + C_n e^{\mu_n c} = (-1)^n \frac{4\pi I}{d^2 \mu_n^2}$$

From these, the coefficient A_n is obtained which is then used to evaluate H_z

$$H_z = \sum_n \left\{ \frac{2\pi I}{d} - (-1)^n \frac{2\pi I}{\mu_n d^2} e^{-\mu_n c} \right\} e^{-\mu_n x} \cos \mu_n z$$

and at the median plane for z = 0

$$H_z = \frac{2\pi I}{d} \sum_n \left\{ 1 - (-1)^n \frac{e^{\mu_n c}}{\mu_n d} \right\} e^{-\mu_n x}$$

The plot of this expression for c = d = 2.5 cm is shown in Fig. 6. In this figure a plot of the field resulting only from the coil is shown for comparison.

One can see clearly that the effect of the plates is to transform the initial field into an exponential one, except (as in Van Bladel's case) near the sources where the r^{-1} dependence tends to dominate.

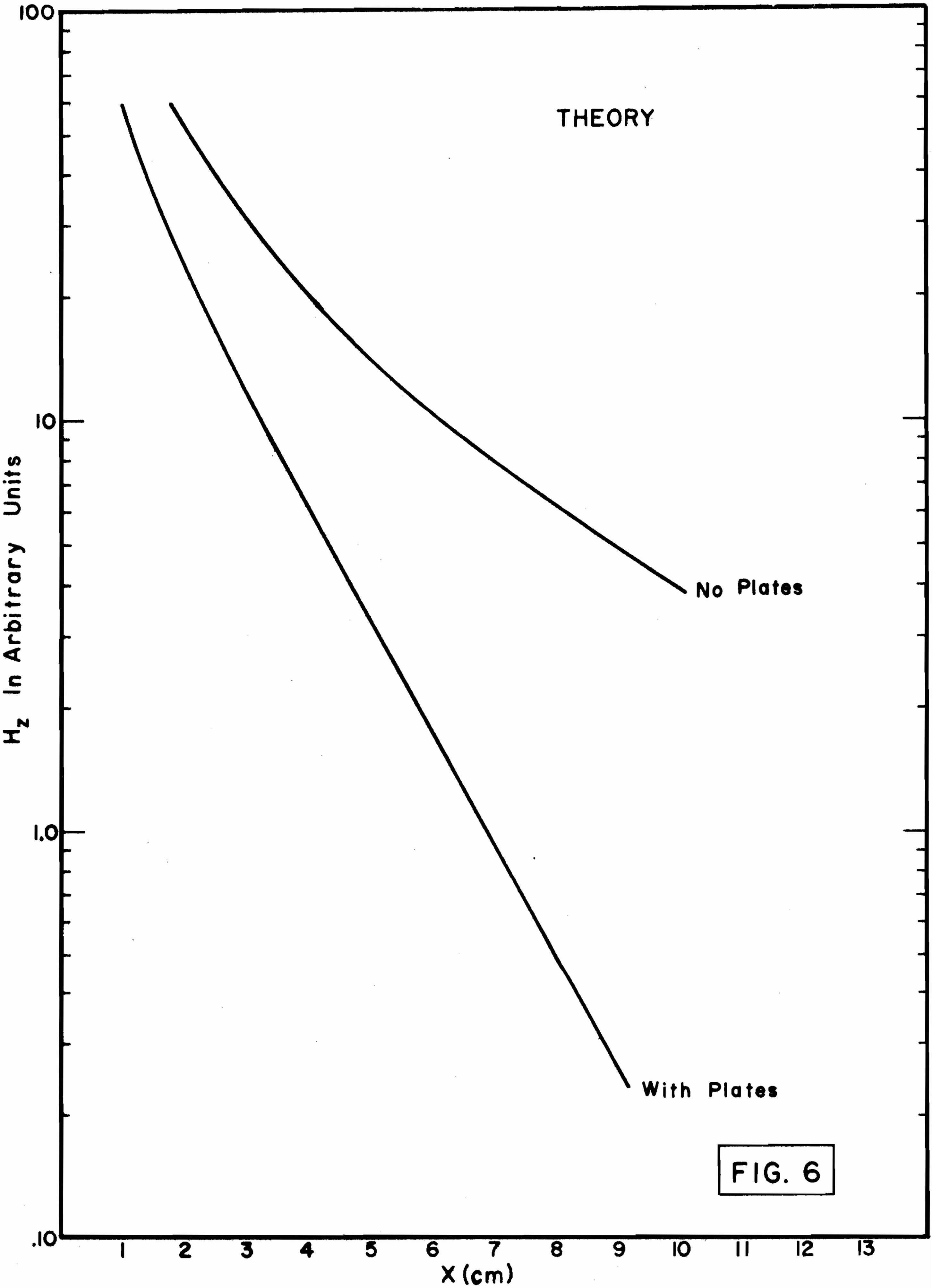
THEORY
100
10
1.0
.10
H_z In Arbitrary Units
No Plates
With Plates
1
2
3
4
5
6
7
8
9
10
11
12
13
X (cm)

FIG. 6

III. EXPERIMENTAL PROCEDURES

A. Analog Magnet

It is known that accurate measurements of magnetic fields at the liquid helium temperature present serious difficulties; thus in order to test experimentally the results outlined above, an analog model was developed. This consisted essentially of a copper coil similar to that shown in Fig. 5, excited by an alternating signal of about 15 kc. The superconducting plates were replaced by copper plates, where the electric skin effect played the role of the Meissner effect in the superconductor. The field at the median plane was measured by means of a small copper coil, free from capacitance coupling, connected to an oscilloscope. The sensitivity of this coil was about 2.1 Oe/V.

A simple test of the experimental arrangement was made. It consisted of measuring the field at the median plane for two equivalent situations, namely, exciting the coil first with direct current, and then with the ac signal and no plates. For the dc measurement a rotating coil was used. It was found that both measurements agree well within the experimental error as can be seen in Fig. 7.

The results of the field measurements when the plates are present appear in Fig. 8. For comparison the results of the theoretical expression for the field with plates are also given. The field values are normalized but in the plot of the theory when plates are present the field is given in arbitrary units. This last curve has been shifted for clarity, and is shown for comparing the slope only. One can see that the theory and the experimental results agree well; however, there is a difference of about 10% in the value of the exponent μ as measured from the graph.

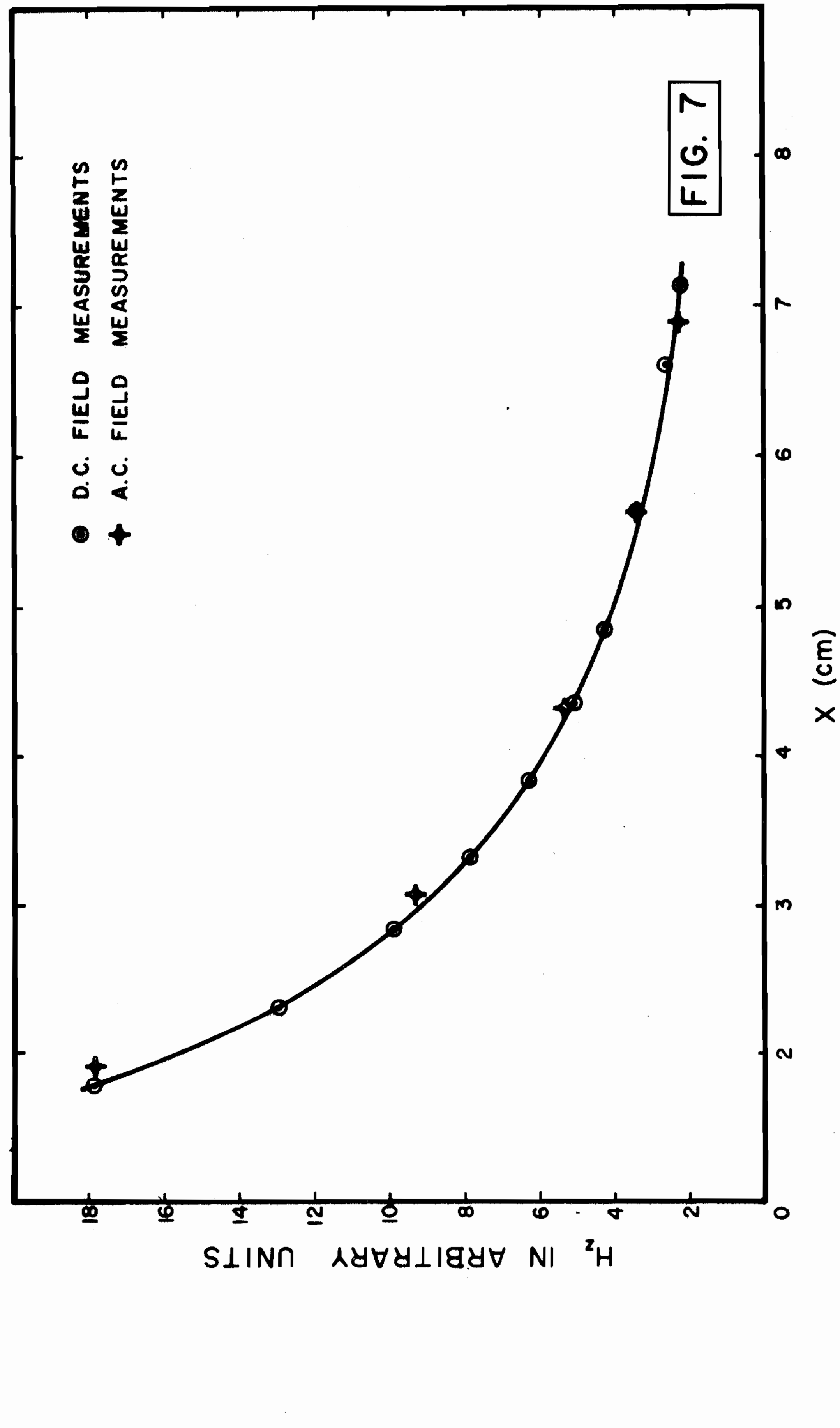
D.C. FIELD MEASUREMENTS
A.C. FIELD MEASUREMENTS
X (cm)
0 2 3 4 5 6 7 8
Hz IN ARBITRARY UNITS
2 4 6 8 10 12 14 16 18

FIG. 7

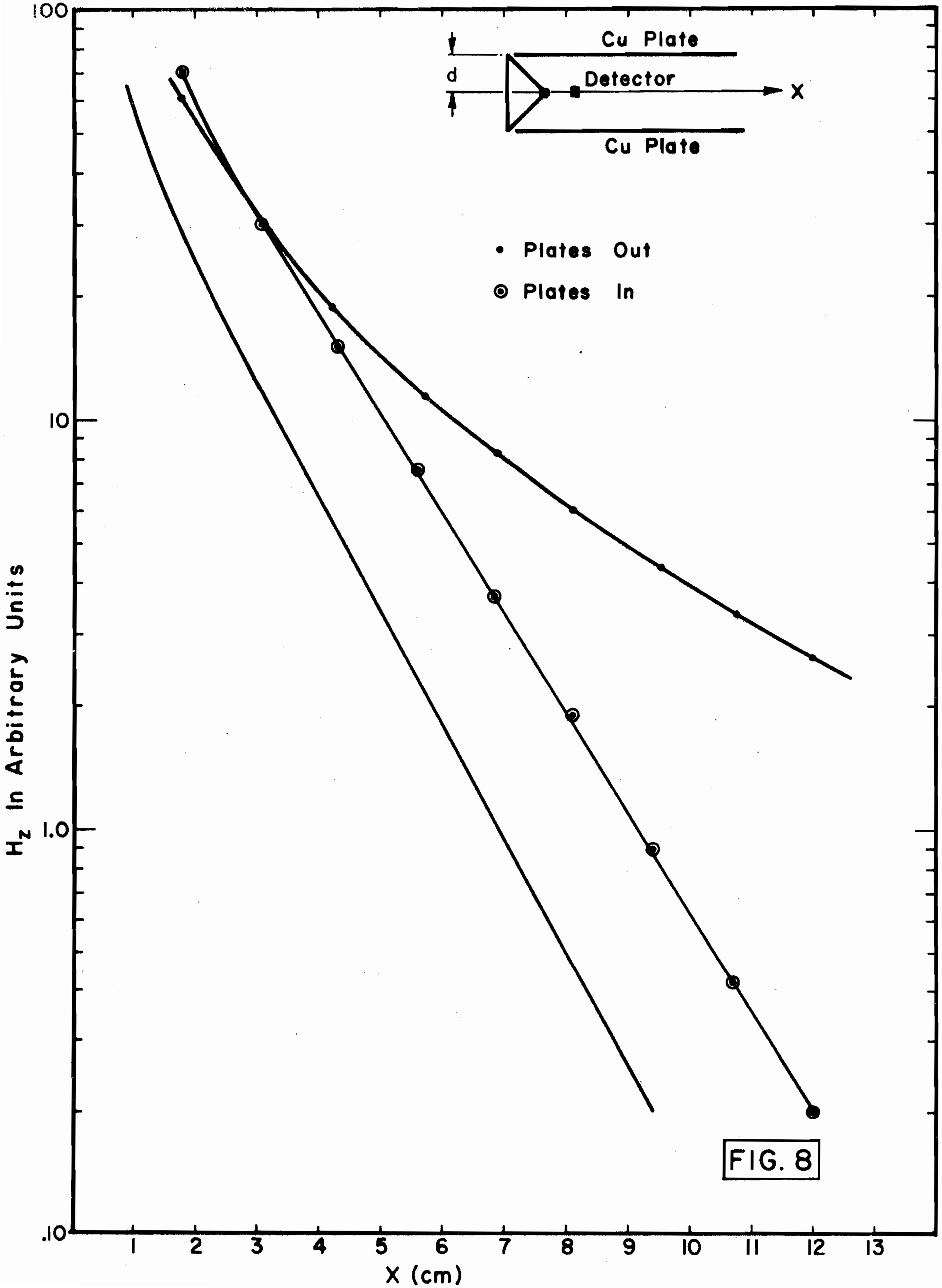
Cu Plate
d
Detector
X
Cu Plate
• Plates Out
◎ Plates In
100
10
1.0
.10
1
2
3
4
5
6
7
8
9
10
11
12
13
H_z In Arbitrary Units
X (cm)

FIG. 8

In a first approximation, μ is a measure of the field index k of an accelerator magnet, and in practice more important than the resulting k value is its constancy at different values of x. We can see from Fig. 9 that the value of μ can easily be changed by varying h, the plate separation, thus allowing the adjustment of k to a desired value. These results also show the range where the exponential dependence is valid.

B. The Superconducting Magnet

i) Cryogenic System: A system, for operating at liquid helium temperatures, large enough to accommodate a superconducting magnet having an approximate volume of five liters, was designed and constructed (see Fig. 10). This consisted of an outer cylindrical metal container, with Santocel insulation, surrounding a liquid nitrogen jacket used to minimize heat losses from the inner helium dewar. The cold helium gas was forced to pass through three heat exchangers, of the Collins type, to cool down three metal plates used both for establishing a temperature gradient along the column and as radiation shields. The power leads feeding current to the magnet were also cooled by the heat exchangers. The heat flow along the column was interrupted by sections of thin wall stainless steel tubing inserted between the heat exchangers. Approximate values of the temperature at the different parts of the column are given in the same figure.

At the bottom of the column, a special bracket was used to support the magnet in a vertical position. The field measuring probe was accurately positioned from the outside top of the dewar, where a vernier scale allowed one to take readings with an accuracy of one thousandth of an inch. The design of the magnet, and the positioning device, was such that errors due to different

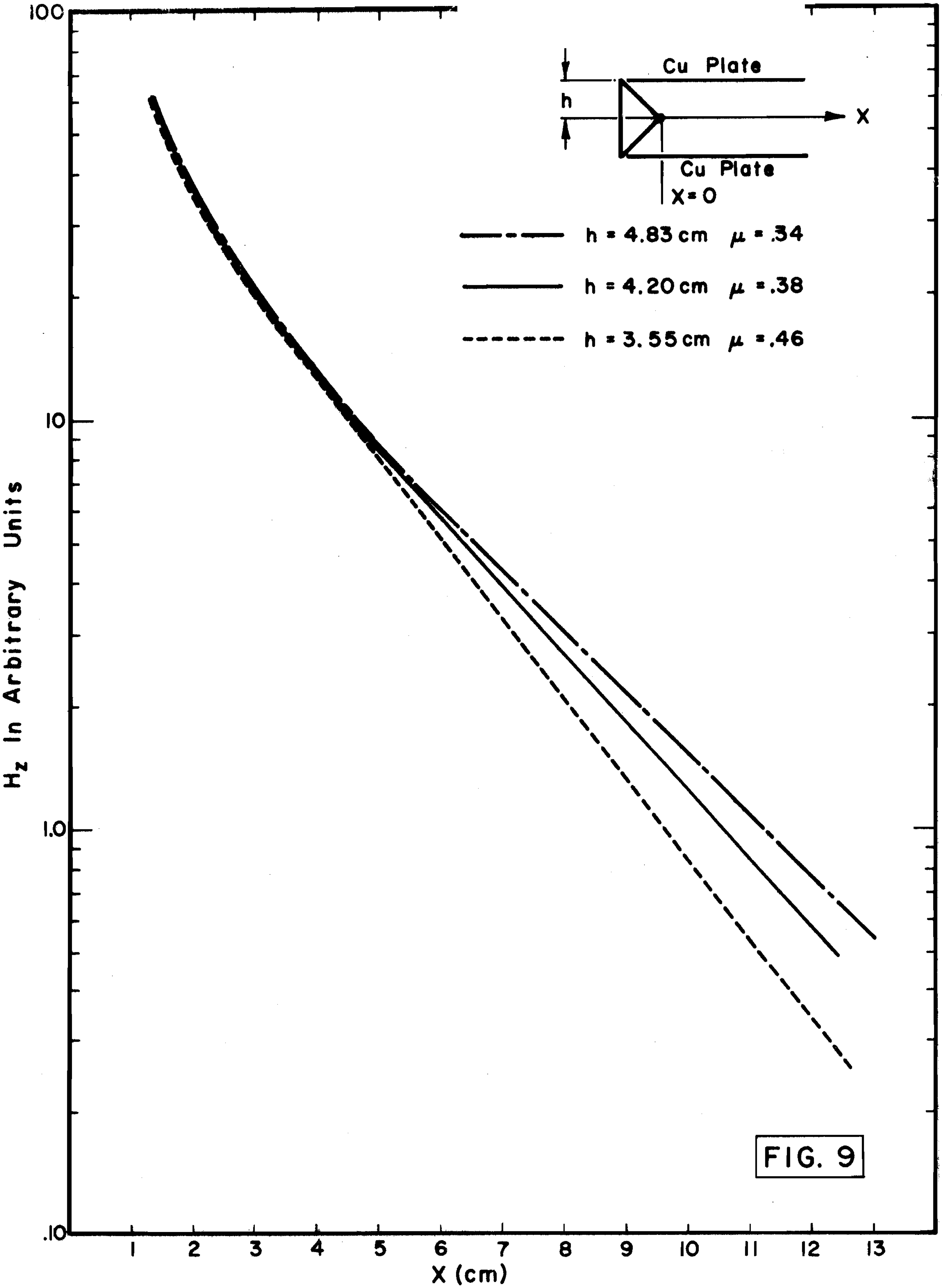

Cu Plate
h
X
Cu Plate
X = 0
h = 4.83 cm μ = .34
h = 4.20 cm μ = .38
h = 3.55 cm μ = .46
100
10
1.0
.10
H_z In Arbitrary Units
1
2
3
4
5
6
7
8
9
10
11
12
13
X (cm)

FIG. 9

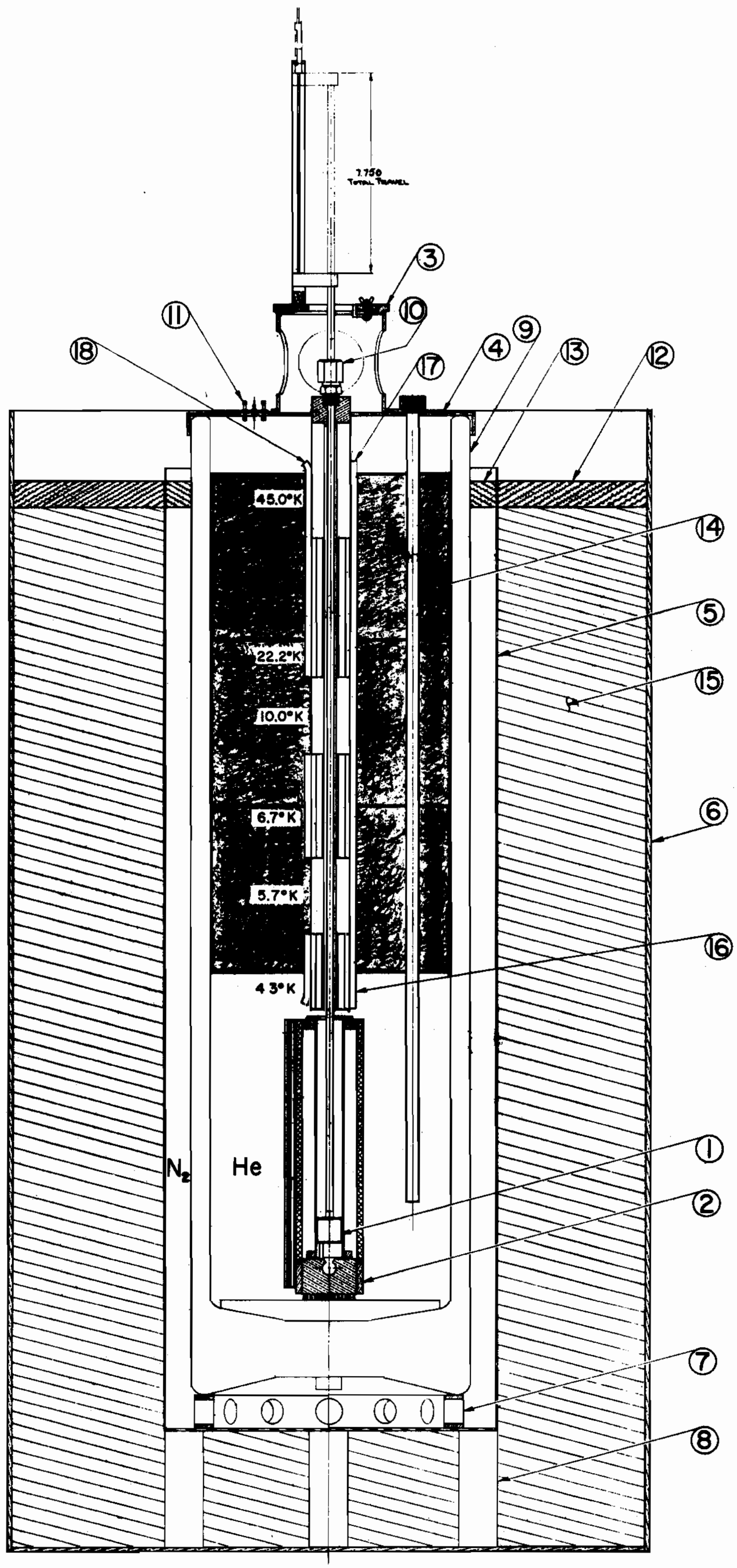

1 Magnetic Probe
2 Magnet & Probe Guide
3 Vertical & Axial Scale Mount
4 H_e Baffel System
5 Inner Container
6 Outer Container
7 Inner Spacer
8 Outer Spacer
9 Liquified Gas Dewer
10 Packing Gland
11 Multi-Terminal Header
12 Styra-foam Insulation Outer
13 Styra-foam Insulation Inner
14 Glass Wool Insulation
15 Santocel Insulation
16 Heat Exchanger
17 Thin Wall Stainless Steel Tube
18 Thin Wall Copper Tube

Fig. 10

thermal expansion of the materials were negligible when the column and the rest of the system were in equilibrium.

The helium evaporation rate, measured when the entire magnet was submerged in liquid amounted to 1.5 liters/hr.

ii) The Field Measuring Probe:[14] It was found that the best way for measuring fields at low temperature was by making use of the magneto-resistance of bismuth fibers. The reasons are the following: The filaments or fibers used as probes are very small in their transverse dimension, about 10 to 25 microns in diameter; also the length can be made small from 2 to 4 mm, thus allowing to measure the field "at a point" when properly oriented in a two-dimensional field. Also the sensitivity and stability of such probes increases at low temperatures.

It is well known, however, that the response of the fibers varies quadratically with the field thus requiring a calibration prior to their use. A small hysteresis and a tendency to saturate at high fields have also been observed. A possible cure for the latter was found in our laboratory and is reported elsewhere.[15]

A standard technique is used to produce a bismuth fiber, namely hot drawing of a soft glass capillary filled with bismuth followed by removal of the glass by means of hydroflouric acid.

The resulting fiber is mounted in a special support as illustrated in Fig. 11. This allows rotation of the fiber around two perpendicular axes, one of them being the longitudinal axis of the fiber. This freedom is necessary, so that one can orient the bismuth crystal structure with respect to the magnetic field so that maximum response is obtained. This corresponded to

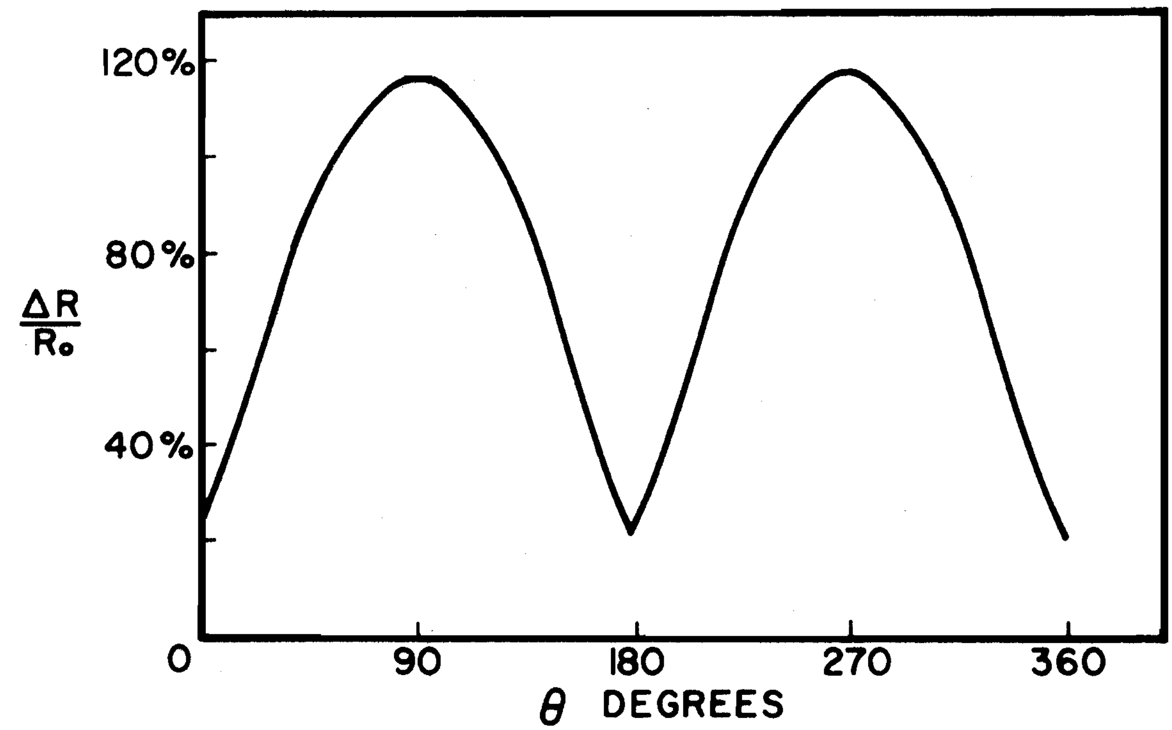
120%
80%
40%
ΔR / Ro
0
90
180
270
360
θ DEGREES

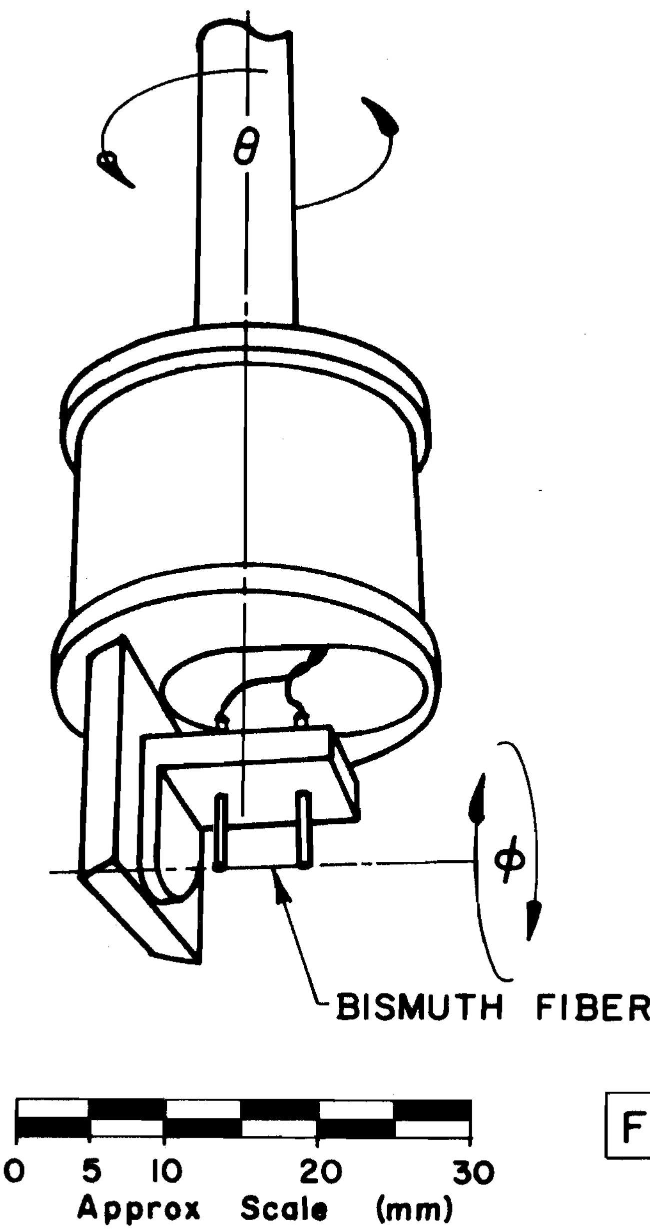
θ
φ
BISMUTH FIBER
0
5
10
20
30
Approx Scale (mm)

FIG. 11

the maximum of the curve shown in Fig. 11. Such orientation also makes the fiber response less sensitive to small angular misalignments.

A typical calibration of a fiber appears in Fig. 12. Due to the observed hysteresis, which amounted to 0.01% to 0.10%, it was necessary, before calibrating a fiber, to expose it to the highest expected field. This operation produced a stabilizing effect which allowed the readings to be reproduced, in some cases, better than one part in ten thousand.

These fibers were handled with great care as they break easily. It was found that a plastic sleeve surrounding the fiber offered good protection against breaking it.

iii) The Magnet: This was made following the dimensions used for the audio-frequency analog. The coil form shown in Fig. 13a was made out of brass; its dimensions were 8-1/2" in the transverse dimension by 2.1" height. The back side was slotted to offer a good support for the winding, which consisted of 2350 turns of 0.005" dia Nb 25% Zr Westinghouse copper cladded superconducting wire with organic insulation. When wound, the conductor could carry about 6.5 amp at 4.2°K.

The plates were machined castings of Wood's metal;[16] their dimensions were 8-1/2 x 11 x 1/4". They were reinforced by a No. 4 stainless steel wire mesh, as previous tests indicated that thermal deformations as large as 0.008" sagging in 4" long samples could occur when using a brass-backed casting. In the reinforced casting, no sagging was observed between room temperature and 77°K. The plates were left to age five months before their use.

A photograph of the magnet is given in Fig. 13b. One can see above the upper plate the terminal strips for connecting the copper wires to the super-

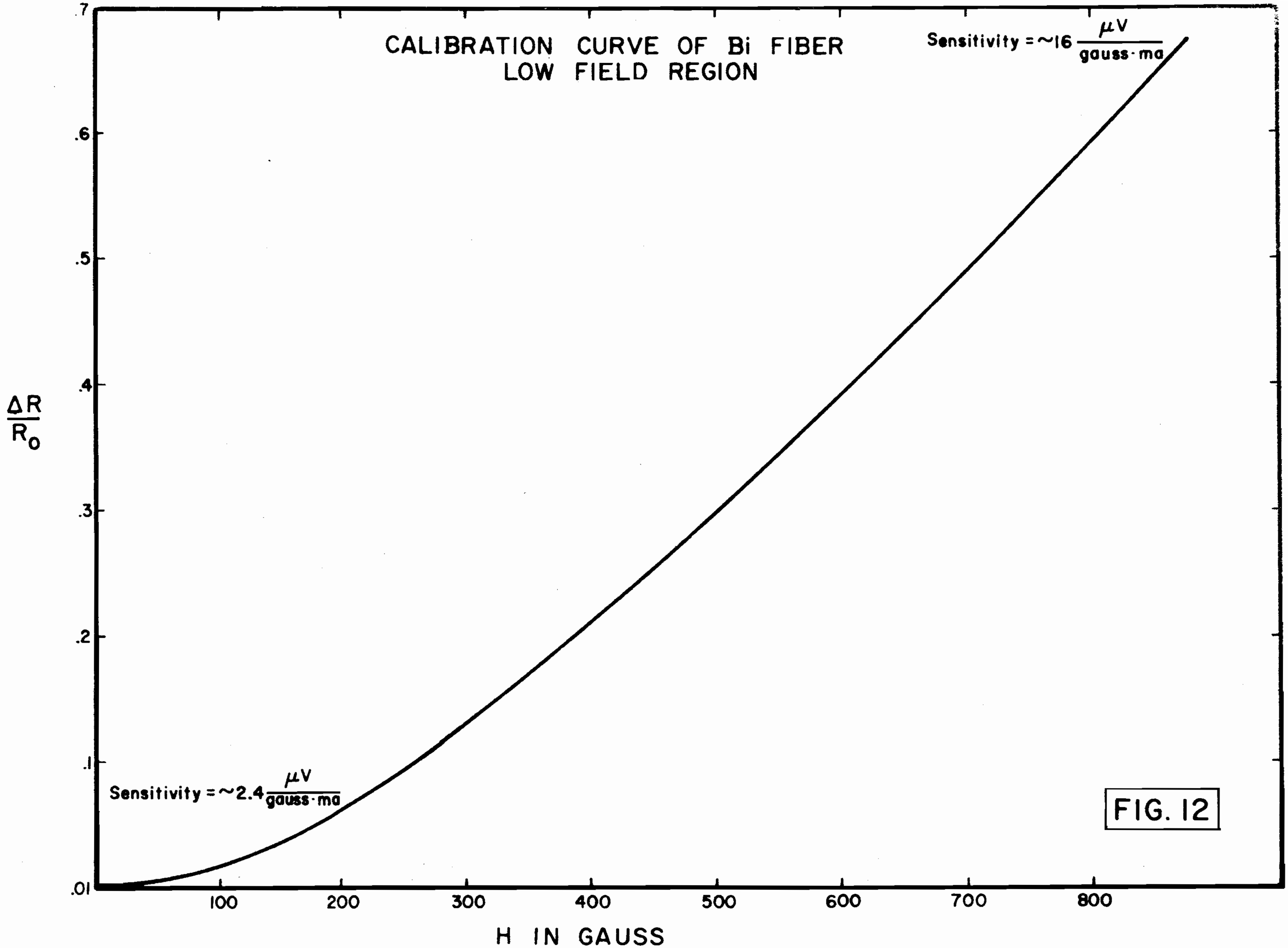
CALIBRATION CURVE OF Bi FIBER
LOW FIELD REGION
Sensitivity = ~16 μV/gauss·ma
Sensitivity = ~2.4 μV/gauss·ma
ΔR/R0
.7
.6
.5
.4
.3
.2
.1
.01
100
200
300
400
500
600
700
800
H IN GAUSS

FIG. 12

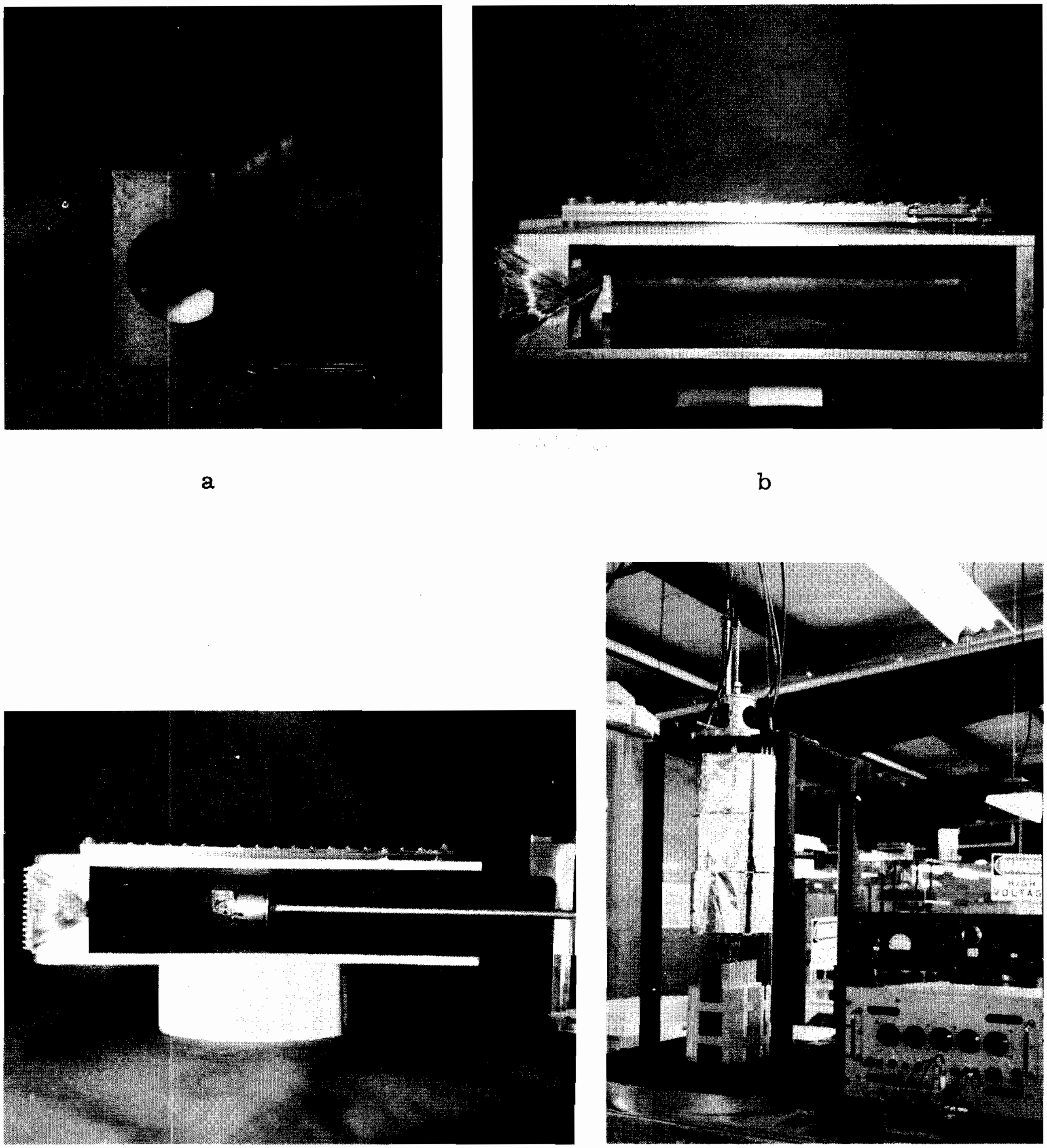

a b c d

Fig. 13

conductor. The tube between the plates was used as a guide for the field measuring probe, which is shown in Fig. 13c, after removing the tube and front supporting plate. Figure 13d shows the magnet assembled in the column together with the probe positioning device; the magnet, in its vertical position, is surrounded by styrofoam blocks to reduce the volume of liquid helium required.

iv) Results: Measurements of the field with and without the superconducting plates were taken at $4.2^{\circ}K$. They showed the same pattern as obtained previously with the audio-frequency analog. These results are shown in Fig. 14 where the plot for the theoretical expression of the field is given for comparison. The value of μ is the same for both.

The results of measurements taken with the plates in place at different excitation currents appear in Fig. 15. One can see a similar behavior in all four cases which indicates that no magnetic flux has penetrated into the superconducting plates. In all these cases the errors in the field measurement amounted to about 1% in the region around 100 gauss and decreased to about 0.1% for the points above 300 gauss.

This raises a question for those points below 50 gauss, where the error seems to be of the order of 50% on the assumption that the exponential law still continues, as indicated by the audio-frequency measurements. From the fiber calibration, the expected error should be of the order of 20 or 30%. Thus, either the field drops down for an unknown reason, or the calibration was unreliable at the low field region. Further meausrements are under way to clarify this point.

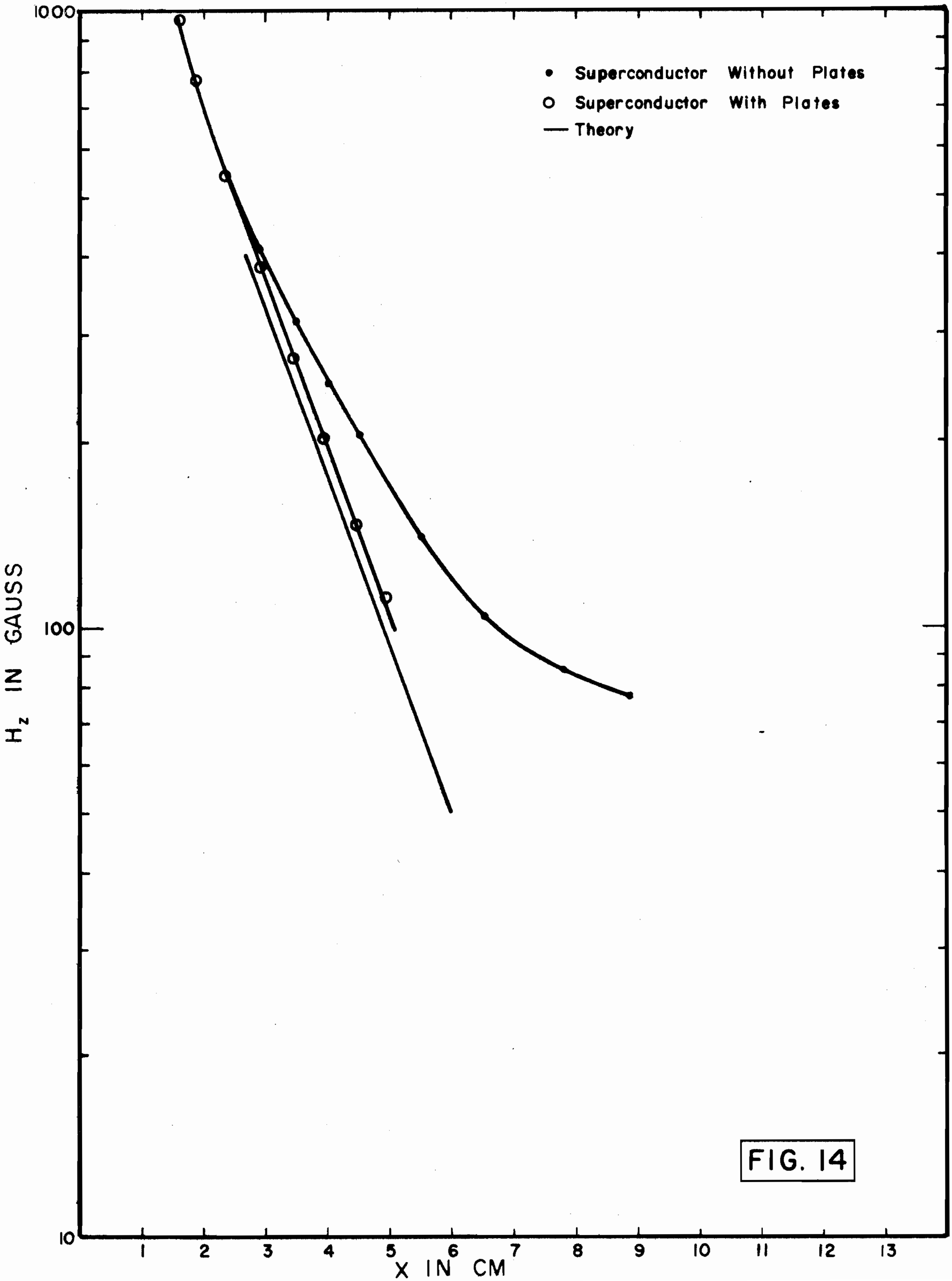
1000
100
10
1
2
3
4
5
6
7
8
9
10
11
12
13
Superconductor Without Plates
Superconductor With Plates
Theory
H_z IN GAUSS
X IN CM

FIG. 14

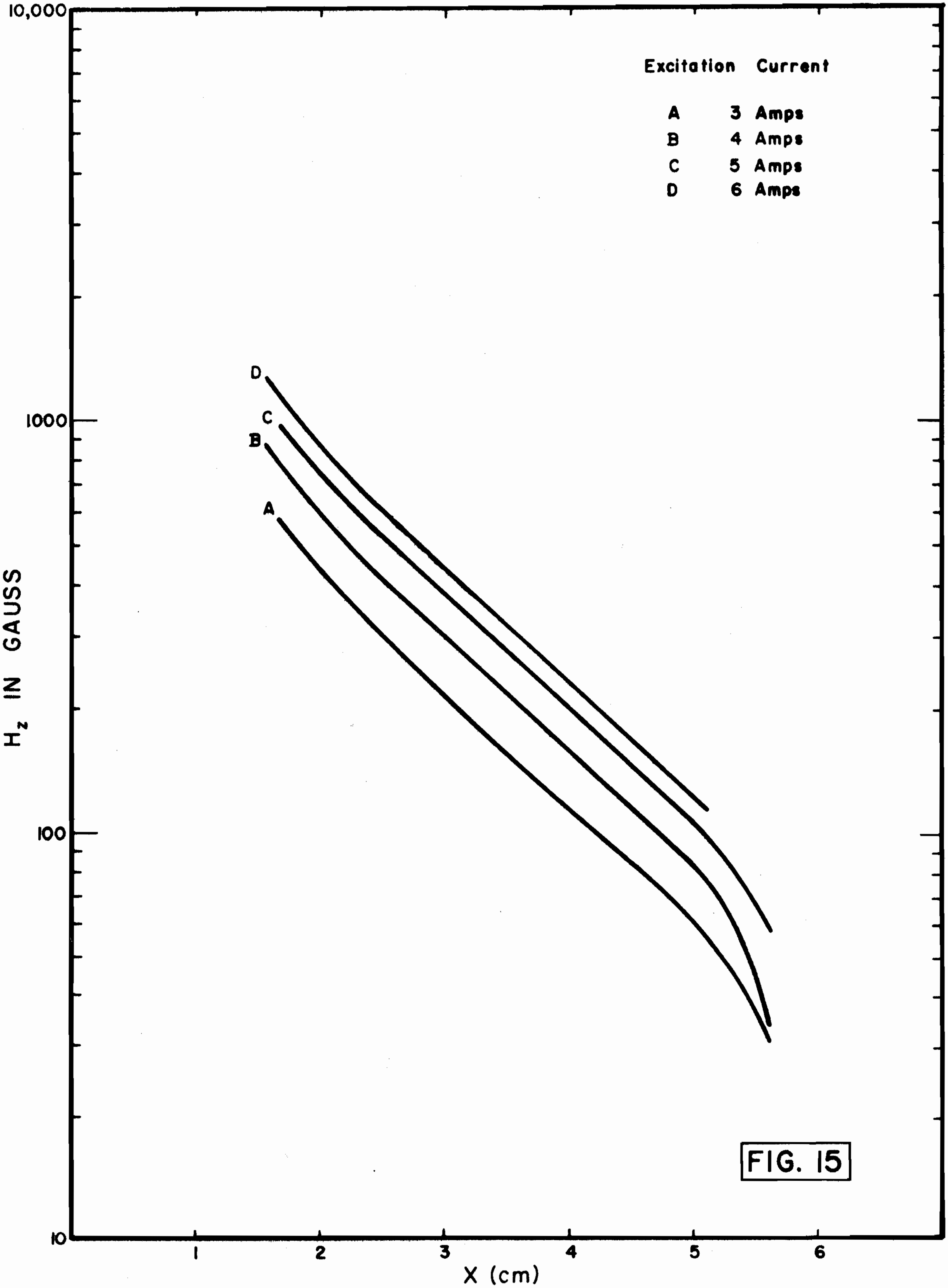
10,000
1000
100
10
H_z IN GAUSS
1
2
3
4
5
6
X (cm)
Excitation Current
A 3 Amps
B 4 Amps
C 5 Amps
D 6 Amps
A
B
C
D

FIG. 15

IV. RECENT DEVELOPMENTS AND CONCLUSIONS

It was mentioned before that the exponential law is changed near the sources, to a degree that it makes the high field region useless for any practical application. This situation is aggravated if one considers that if such magnet is used in an accelerator, the beam would be moving in the same plane of the superconducting bundle, making impractical a simple beam extracting mechanism.

A solution of both problems was found by splitting the coil into two coils symmetrically located above and below the median plane. This arrangement has some resemblance to the case studied by Van Bladel as shown in Fig. 2. A sketch of this "geometry" and the results obtained from the audio-frequency analog appear in Fig. 16. Two graphs are given, one corresponding to parallel plates and a second one showing an exponential behavior obtained by tilting the plates.

Further studies made in the analog demonstrated that "on the spot" adjustments of the magnet parameters can be made by changing the separation and inclination of the plates. This split coil arrangement offered, among other things, a field reversal at negative values of x, desirable for extraction purposes.

The field variation in the transverse direction (Y axis) was determined, for a single coil geometry, by the analog magnet method. These results can be seen in Fig. 17. The measurements were taken at different distances from the center bundle ($x = 0$). The scale for the curve $x \approx 4$ cm has been reduced 0.5 times to fit the size of the graph. The flattening of the field produced by the plates is clearly shown in the curves marked $x = 10$ and 17 cm. The

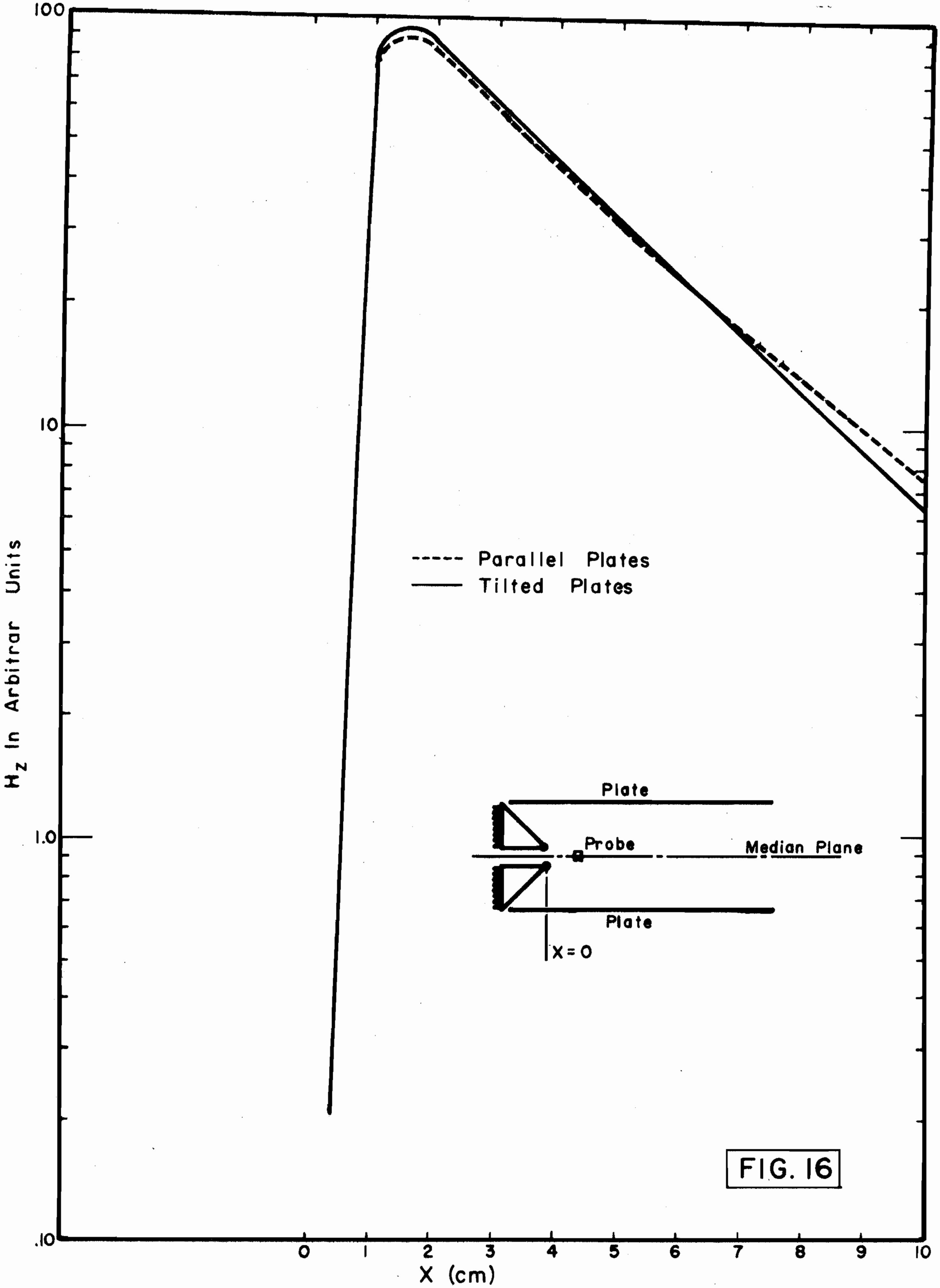

100
10
1.0
.10
H_z In Arbitrar Units
0
1
2
3
4
5
6
7
8
9
10
X (cm)
Parallel Plates
Tilted Plates
Plate
Probe
Median Plane
Plate
X=0

FIG. 16

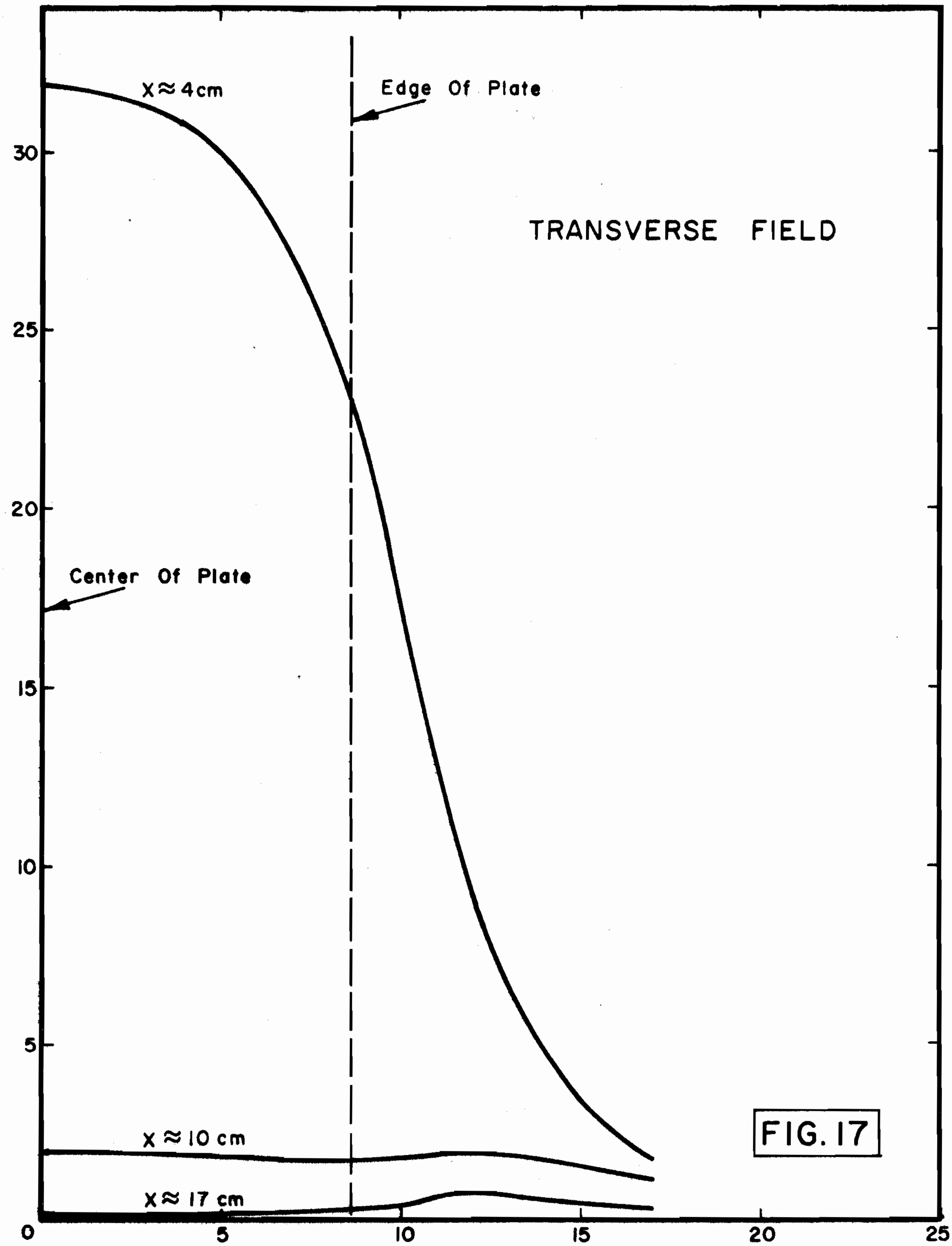

X ≈ 4cm
Edge Of Plate
TRANSVERSE FIELD
Center Of Plate
X ≈ 10 cm
X ≈ 17 cm
30
25
20
15
10
5
0
5
10
15
20
25

FIG. 17

slight raise beyond the edge of the plates can be interpreted as produced by the sides of the coil, or the circulating current in the edge of the plates, or possibly a combination of both.

One may conclude that the results of this work indicate that it is possible to shape a magnetic field by using superconducting surfaces. The assumption that the magnetic field is excluded from the superconducting plates is valid for the fields described in this work. It is also demonstrated that in a first approximation modeling studies can be done by using an audio-frequency model, with a high conductivity metal playing the role of the superconducting surfaces.

V. ACKNOWLEDGEMENTS

The author wants to thank Professor J. D. Dillinger of the University of Wisconsin for his continuous help and valuable suggestions in the design of the low temperature components described in this paper. Many hours of difficult and tedious calibration work were patiently spent by him in the course of this investigation. Very valuable help in the theoretical aspect came from Dr. S. C. Snowdon of the MURA staff. Equally valuable was the help received from Dr. R. W. Fast of MURA in taking measurements and discussing the results.

VI. REFERENCES

1. Reference to the early work in superconductivity is made in a book by D. Shoenberg, SUPERCONDUCTIVITY, Cambridge University Press 1960, p. 37.
2. J. E. Kunzler, E. Buehler, F. S. L. Hsu and J. H. Wernick, Phys. Rev. Letters 6, 89 (1961).
3. T. G. Berlincourt, R. R. Hake and D. H. Leslie, Phys. Rev. Letters 6, 671 (1961).
4. K. R. Symon, D. W. Kerst, L. W. Jones, L. J. Laslett and K. M. Terwilliger, Phys. Rev. 103, 1837 (1956).
5. S. C. Snowdon, R. S. Christian, G. del Castillo and R. W. Fast, Proc. International Conference on High Energy Accelerators (Dubna, 1963), p. 578.
6. A very complete review of the present work is given in Rev. Mod. Phys. 36, 1 - 328 (1964).
7. E. R. Shrader and F. Kolondra, The RCA Review, Vol. 25, p. 582 (1964).
8. P. de Feo and G. Sacerdoti, Phys. Letters 2, 264 (1962)
9. R. Babcock and H. Riemersma, Appl. Phys. Letters 1, 43 (1962).
10. N. Cabibbo and S. Doniach, Phys. Letters 4, 29 (1963)
11. A collection of papers regarding this accelerator is given by the MURA Staff in Rev. Sci. Instr. 35, 1393 (1964).
12. J. Van Bladel, MURA Technical Notes Nos. 322 and 327 (1962, unpublished).
13. K. R. Symon, BNL (T-290), p. 162 (1962).
14. Part of this section was published by the author in BNL 7534, p. 449 (1963).
15. G. del Castillo and R. W. Fast, to be published in J. of Appl. Phys.
16. Cerrobend 158 - Cerro de Pasco Sales Corp., New York 22, New York.